First order perturbative calculations for a conducting liquid jet in a solenoid
DRAFT 2

J. Gallardo, S. Kahn, R.B. Palmer, P. Thieberger, R. Weggel
Brookhaven National Laboratory

K. McDonald
Princeton University

February 25, 2002

Abstract

A perturbative calculation is given of the behavior of a continuous jet of conducting fluid as it enters and leaves a solenoidal magnetic field. It is assumed that the changes in direction, jet cross section and velocity are small.

If the jet enters the field along, or close to the axis, then the induced forces are compressive and retarding. The jet slows, suffers an increase in hydrostatic pressure, and increases in diameter; later, the jet re accelerates and shrinks. As the jet leaves the field, the hydrostatic pressure becomes negative and cavitation may occur.

If the jet enters at an angle to the axis, there are, in addition, deflections and elliptical deformations of the jet.

Formulas are given for these effects and numerical values given for the example of a solenoidal field with a Gaussian axial profile.

Contents

1 Introduction

A mercury jet, injected at an angle respect to the axis of the solenoidal field, is the current baseline solution for the Feasibility Study II[1]. The interaction of the liquid-metal jet with the strong 20 T target solenoid has as result a number of forces on the jet which potentially may affect the viability of this target.[2],[3],[4] We present here perturbative calculations which confirm the findings of previous authors.

2 Formulas

2.1 Introduction

The jet is assumed to have an initial radius r, and be traveling at a velocity v. Changes in radius, shape, direction and velocity are all assumed to be small. The angle between the jet and solenoid axes is also assumed to be small.

No viscosity

$r << L$

In the following formulas, the coordinate system is defined by the jet; z is along the direction of motion and r is perpendicular to z.

If the jet is not directed along the solenoid axis, then we also define y in a direction perpendicular to z (the jet axis) and away from the solenoid axis; and x perpendicular to y and z; and we define a second coordinate system $x\ y'\ \ z'$, where z' is aligned along the magnet axis. Assuming a small angle $\theta^2 << 1$ then (See fig. 1):

$$x' \approx x$$

,

$$y' \approx y_o + z\,\theta$$

,

$$r'^2 \;\approx\; r^2 \;+\; 2z\; y_o\; \theta$$

,

$$z' \;\approx\; z - y_o$$

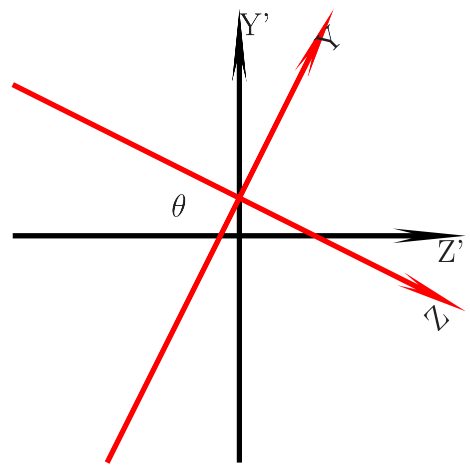

6cm Figure 1: Schematic of the geometric arrangement of solenoid and jet

2.2 Induced azimuthal current

The magnetic flux through a circle of radius r perpendicular to the jet axis is

$$\Phi = \int_S dS\vec{n} \cdot \vec{B} \approx \pi r^2 B_z(x, y, z) \tag{1}$$

As a liquid metal jet passes axially down such a field at a velocity $v = dz/dt$, a circumferential potential will be generated[6]

$$V \equiv \oint \vec{E} \cdot d\vec{l} = -\frac{d\Phi}{dt} = \pi r^2 v \frac{dB_z(x, y, z)}{dz} \tag{2}$$

If the metal electrical conductivity σ is low enough so that the resulting current has a negligible effect on the field, then the azimuthal current density i_ϕ will be

$$i_\phi \approx \frac{V}{2\pi r}\sigma \tag{3}$$

$$i_\phi \approx \frac{rv\kappa}{2} \frac{dB_z(0, 0, z)}{dz} \tag{4}$$

2.3 Radial forces and Hydrostatic pressure

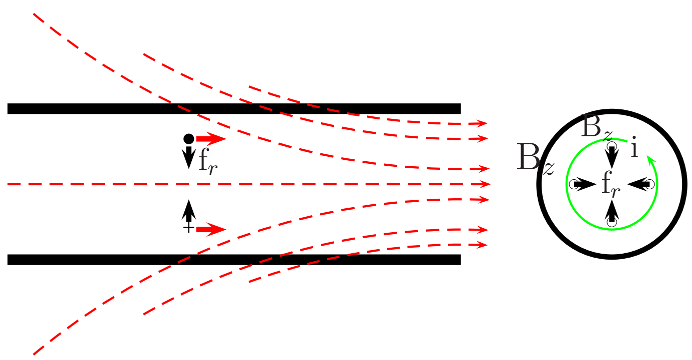

Figure 2: Presure force in the axial case

The induced radial force per unit volume ($dr\ r\ d\phi dz$) is

$$f_r = B_z i_\phi \approx \frac{r}{2}\ v\kappa\ B_z \frac{dB_z}{dz} \tag{5}$$

If we assume the effects of the fields are small so that the jet radius and liquid velocities do not vary by large fractions, and if we ignore radial inertia, then the hydrostatic pressures in a jet of outside radius r_o, at radius r, will be given by

$$p(r,z) = \int_{r_o}^{r} -f_r dr \approx \left(\frac{r_o^2 - r^2}{4}\right)\ v\kappa\ B_z \frac{dB_z}{dz} \tag{6}$$

2.4 Axial force

The above hydrostatic pressure is a function of z, and gradients in it will exert axial pressures f_p on the liquid that must be added to the magnetic term f_z(hydrostatic).

$$f_p(\text{hydrostatic}) = \frac{dp(r,z)}{dz} \approx\ -\ \left(\frac{r_o^2 - r^2}{4}\right)\ v\kappa\ \frac{d}{dz}\left(B_z \frac{dB_z}{dz}\right) \tag{7}$$

To this must be added the axial forces induced directly by the fields acting on the azimuthal currents:

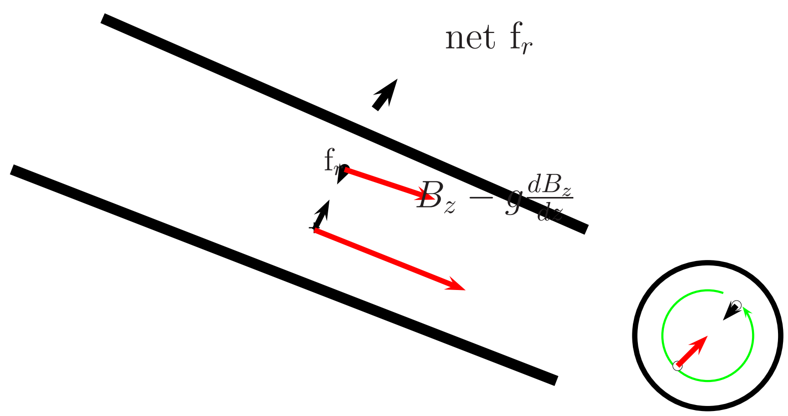

Figure 3: Deflection in the tilded case

If the jet is aligned with the field axis ($\theta = 0$, the radial field is given by

$$B_r(\theta = 0) \approx -\frac{r}{2}\frac{\partial B_z(0,0,z)}{\partial z} \tag{8}$$

The induced axial force per unit volume ($dr\ d\phi\ dz$) is

$$f_z(\theta = 0) \ = \ f_p(r,z) \ - \ B_r i_\phi$$

If the jet is at an able to the magnetic axis, then there is an additional shear force:

$$f_z(\theta) \ = \ f_p(r,z) \ - \ B_y i_\phi \ \sin(\phi)$$

giving, in all:

$$f_z \ \approx \ - \left(\frac{r_o^2 - r^2}{4}\right) \ v\kappa \ \frac{d}{dz}\left(B_z \frac{dB_z}{dz}\right) \ + \frac{r^2}{4} v\kappa \left(\frac{dB_z}{dz}\right)^2 \ + \ \frac{rv\kappa}{2} \ B_y \ \frac{dB_z}{dz} \sin(\phi) \tag{9}$$

On the jet axis:

$$f_z \ \approx \ - \ \left(\frac{r_o^2}{4}\right) \ v\kappa \ \frac{d}{dz}\left(B_z \frac{dB_z}{dz}\right) \tag{10}$$

On the outer surface, averaged over the azimuthal angle ϕ, or in the absence of a B_y:

$$f_z \ \approx \ \frac{d}{dz}\left(B_z \frac{dB_z}{dz}\right) \ + \ \frac{r^2}{4} v\kappa \left(\frac{dB_z}{dz}\right)^2 \tag{11}$$

On the outer surface, with a finite B_y, as in the case of a jet at an angle to the magnetic axis:

$$f_z \ \approx \ \frac{d}{dz}\left(B_z \frac{dB_z}{dz}\right) \ + \ \frac{r_o^2}{4} v\kappa \left(\frac{dB_z}{dz}\right)^2 \ + \ \frac{yv\kappa}{2} \ B_y \ \frac{dB_z}{dz} \tag{12}$$

and the average force of the disk of radius r_o is given by integrating the terms

$$< f_z > \approx \frac{r_o^2}{8} v\kappa \left(\left(\frac{dB_z}{dz}\right)^2 \ + \ \frac{d}{dz}\left(B_z \ \frac{dB_z}{dz}\right)\right) \tag{13}$$

2.5 Axial accelerations

These forces will then decelerate, or accelerate layers of the fluid, thus inducing differences of liquid velocity as a function of radius

$$\frac{dv}{dz} \ = \ \frac{f}{\rho \ v} \tag{14}$$

$$\Delta \ v(r,z) \ = \ \int_{z_o}^{z} (f_z + f_p) \ \frac{1}{v\rho} \ dz \tag{15}$$

The average change in velocity is then

$$< \Delta v > (z) \;=\; \frac{\kappa}{\rho}\;\frac{r_o^2}{8}\;\left(\int_{z_o}^{z}\left(\frac{dB_z}{dz}\right)^2 \;+\; \frac{d}{dz}\left(B_z\frac{dB_z}{dz}\right)\;dz\right) \tag{16}$$

and the radius as a function of z is

$$r(z) \;=\; r_o\;\left(1\;-\;\frac{< \Delta v > (z)}{v}\right) \tag{17}$$

2.6 Transverse forces and deflections

¿From above, the radial force per unit volume ($dr\ r\ d\phi dz$) is

$$f_r = B_z i_\phi \approx \frac{r}{2}\;v\kappa\;B_z\frac{dB_z}{dz} \tag{18}$$

If B_z varies with a transverse distance y, then the component of this radial force in the y direction is

$$f_y = f_r\;\sin\phi \tag{19}$$

and the net deflective force dF_y per unit length dz is

$$\frac{dF_y}{dz} \;=\; \int_o^r\;\int_o^{2\pi}\frac{r}{2}\;v\kappa\;\frac{dB_z}{dy}\;r\sin\phi^2\frac{dB_z}{dz}\;r\;drd\phi \tag{20}$$

$$=\;\frac{v\kappa}{2}\;\frac{dB_z}{dy}\;\frac{dB_z}{dz}\;\int_o^{2\pi}\sin\phi^2 d\phi\int_o^r r^3\;dr \tag{21}$$

$$=\;\frac{\pi}{8}v\kappa\;r^4\;\frac{dB_z}{dy}\;\frac{dB_z}{dz} \tag{22}$$

and the change in transverse velocity

$$\begin{aligned}\frac{dv_y}{dz} \;&=\; \frac{1}{v}\frac{dv_y}{dt}\\ &=\; \frac{\frac{dF_y}{dz}dz}{v\rho\pi r^2 dz}\\ &=\; \frac{\kappa r^2}{8\rho}\frac{dB_z}{dy}\frac{dB_z}{dz}\end{aligned}$$

and the inverse radius of bend is

$$\frac{d^2y}{dz^2} \;=\; \frac{d\theta}{dz} \;=\; \frac{\kappa\;r^2}{8\;v\;\rho}\;\frac{dB_z}{dy}\;\frac{dB_z}{dz} \tag{23}$$

Figure 4: Induced axial currents

2.7 Induced axial current

The magnetic flux between transverse positions $-x$ to x and dz is

$$d\Phi_y = 2xdzB_y(z) \tag{24}$$

As a liquid metal jet passes axially down such a field at a velocity $v = dz/dt$, axial voltage gradients will be generated

$$G = x\frac{dB_y}{dz}v \tag{25}$$

If the metal electrical conductivity κ is low enough so that the resulting current has a negligible effect on the field, then the axial current density i_z will be

$$i_z = G\sigma \tag{26}$$

$$i_z \;= xv\kappa\frac{dB_y(0,0,z)}{dz} \tag{27}$$

2.8 Transverse elliptical distortion

If the jet is not on the solenoid axis, the axial induced currents interacting with the transverse fields will generate distorting forces on the jet. These transverse forces per unit volume $dx\ dy\ dz$ are

$$f_x \;=\; i_z\ B_y \;=\; x\ v\ \kappa\ B_y\ \frac{dB_y}{dz} \tag{28}$$

This force will distort the cross section. Assuming that the liquid in incompresible, we must find the induced pressures and motions $\Delta\vec{r}$ within the cross section that are driven by this force, with the constraint that the divergence of these motions is zero:

$$Div(\Delta\vec{r}) \;=\; 0$$

Defining

$$F_o \;=\; v\ \kappa\ B_y\ \frac{dB_y}{dz}$$

so that the magnet force per unit volume:

$$f_x(\text{magnetic}) \;=\; x\ F_o$$

2.8.1 Magnetic Forces

The pressure on the surface of the jet will be independent of azimuth ϕ:

$$p(r_o)_{\mathrm{circular}} = p_{\mathrm{atm}} \; + \; T/r_o \; ,$$

T being the surface tension. If the initial cross section is circular, we can consider pressures within the cross section:

$$p \; = \; p_o \; - \; r^2 \; \frac{F_o}{4}$$

where p_o is set by the constraint the above surface pressure at $r = r_o$. This bulk pressure will induce radial pressure forces:

$$f_r(\mathrm{pressure}) \; = \; \frac{dp}{dr} \; = \; - \; \frac{r \; F_o}{2}$$

so

$$f_x(\mathrm{total}) \; = \; F_o \; \left(x \; - \; \frac{r \; \cos(\phi)}{2} \right) \; = \; \frac{x \; F_o}{2}$$

$$f_y(\mathrm{total}) \; = \; - \; \frac{F_o \; r \; \sin(\phi)}{2} \; = \; - \; \frac{y \; F_o}{2}$$

and the accelerations:

$$\frac{d^2 x, y}{dz^2} \; = \; \frac{f_{x,y}}{v \; \rho}$$

will give displacements:

$$\Delta x \; = \; \int \int \frac{f_{x,y}}{v \; \rho} \; dz^2 \; = \; x \; \frac{\kappa}{2 \; \rho} \; \int \int \; B_y \; \frac{dB_y}{dz} \; dz^2$$

$$\Delta y \; = \; \int \int \frac{f_{x,y}}{v \; \rho} \; dz^2 \; = \; - \, y \; \frac{\kappa}{2 \; \rho} \; \int \int \; B_y \; \frac{dB_y}{dz} \; dz^2$$

Such motions are quadrupole (see fig ***) and, as required, give $Div \; (dx, dy) \; = \; 0$. The resulting ellipticity $\epsilon = \frac{\Delta x_o}{r_o} \; = \; - \frac{\Delta y_o}{r_o}$:

$$\epsilon(z) \; = \; \frac{r_o \; \kappa}{2 \; \rho} \; \int \int B_y \; \frac{dB_y}{dz} \; dz^2 \tag{29}$$

Figure 5: Surface tension forces

2.8.2 Surface Tension Forces

Once the cross section becomes somewhat elliptical (we consider only a small ellipticity), then the pressure at the surface is no longer independent of the azimuthal angle ϕ, but is given by:

$$p(r = r_o) \;=\; p_{\text{atm}} \;+\; \frac{T}{r_0}\;(1 \;-\; \epsilon)\; \cos(2\;\phi)$$

Consider, in addition to those given above for the circular case, pressures within the cross section:

$$p(x, y)_{\text{elliptical}} \;=\; p_o \;+\; \frac{T\;\epsilon}{r_o}\;\left(\cos^2(2\;\phi) \;-\; \sin^2(2\;\phi)\right) \;=\; p_o \;+\; \frac{T\;\epsilon}{r_o^3}\;(x^2 \;-\; y^2)$$

which has the correct values at $r = r_o$.

Defining

$$S_o \;=\; \frac{2\;T\;\epsilon}{r_o^3},$$

the resulting bulk forces are:

$$f_x(\text{elliptical}) \;=\; \frac{dp}{dx} \;=\; x\;S_o$$
$$f_y(\text{elliptical}) \;=\; \frac{dp}{dy} \;=\; -\,y\;S_o$$

which are, once again, quadrupole forces that will generate quadrupole motions with Div($\vec{dr}$)=0.

$$\Delta x, \Delta y \;=\; \int\!\!\int \frac{(x, \;\; -\,y)}{v\;\rho}\;S_o\;dz^2$$

2.8.3 Magnetic and Surface Tension Forces

Adding these surface tension displacements to the forces derived for the circular case:

$$\Delta x, \Delta y \;=\; (x, \;\; -\,y)\;\int\!\!\int\left(\frac{\kappa}{2\;\rho}\;B_y\;\frac{dB_y}{dz} \;+\; \frac{2\;T\;\epsilon}{v\;\rho\;r_o^3}\right)\;dz^2$$

and the resulting ellipticity $\epsilon = \frac{\Delta x_o}{r_o} \;=\; -\,\frac{\Delta y_o}{r_o}$:

$$\epsilon(z) \;=\; \int\!\!\int\left(\frac{r_o\;\kappa}{2\;\rho}\;B_y\;\frac{dB_y}{dz} \;+\; \frac{2\;T\;\epsilon}{v\;\rho\;r_o^2}\right)\;dz^2 \tag{30}$$

3 Gaussian Case

We can consider a field that varies as a Gaussian in z The fields of the solenoid and coordinates are denoted with primes ($'$).

The Fields in the magnet system are:

$$B'_z(r',z') \approx B_o e^{-\frac{z'^2}{2\sigma_z^2}} - \frac{1}{4} r'^2 \frac{\partial^2 B'_z(0,z')}{\partial z'^2} \quad (31)$$

$$B'_r(r',z') \approx -\frac{1}{2} r' \frac{\partial B'_z(0,z')}{\partial z'} \quad (32)$$

In the coordinate system of the jet, see Fig. 1, assuming a very small angle θ then $x' = x$, $y' = y_o + z\theta$, $r'^2 = r^2 + 2zy_o\theta$ and $z' = z - y_o\theta$ and the fields are

$$\begin{aligned}
B_z(x,y,z) &\approx \left[B'_z(r',z') - \frac{1}{2}\theta\ y_o\ \frac{\partial B'_z(0,z')}{\partial z'} \right] \\
B_x(x,y,z) &\approx -\frac{1}{2} x \frac{\partial B'_z(0,z')}{\partial z'} \\
B_y(x,y,z) &\approx -\left[\frac{1}{2}(\ y_o\ + z\theta) \frac{\partial B'_z(0,z')}{\partial z'} - \theta B'_z(r',z') \right] \\
\frac{\partial B_z(x,y,z)}{\partial z} &\approx \left[\frac{\partial B'_z(0,z')}{\partial z'} - \frac{1}{2}\ y_o\ \theta \frac{\partial^2 B'_z(0,z')}{\partial z'^2} \right] \\
\frac{dB_y(x,y,z)}{dz} &\approx \left[\frac{1}{2}\theta \frac{\partial B'_z(0,z')}{\partial z'} - \frac{1}{2}(\ y_o\ + z\theta) \frac{\partial^2 B'_z(0,z')}{\partial z'^2} \right] \quad (33)
\end{aligned}$$

4 Study 2 Example

In the Study 2 target system, the beam with rms radius σ_r intersects a mercury jet of radius r_o at an angle $\theta_{crossing}$. The forward velocity of the jet is v_o. The intervals between pulses is t, and it will be assumed here that after a pulse, all the mercury outside of the nozzle is dispersed. The nozzle is at z_{nozzel} with respect to the intersection of the beam and jet center lines. Consider the following parameters:

σ_r	1.5	mm
r_o	5	mm
$\theta_{crossing}$	33	mrad
v_o	30	m/sec
t	20	ms
z_{nozzel}	-.375	m

The distribution of resulting interactions as a function of z is shown above. At the time of a second, or subsequent bunch, the newly established jet will

Figure 6: Write caption

extend a distance $z_{jet} = v_o\, t = 0.6$ m from the nozzle. It is seen that only 2.5 % of the interactions would occur after this location, had the beam extended indefinitely. Thus there is a negligible loss from this limited jet extent.

Thus the total length over which the jet must propagate without serious magnetic disruption is from the nozzle to a point 0.6 m downstream. In order to minimize the field non uniformity over this length, the magnetic center (approximate point of maximum B_z is placed at the center of this length. i.e. the magnetic center is set at a distance $z_{magnet} = z_{jet}/2 - z_{nozzel} = \ -.15$ m with respect to the jet-beam intersection. the figures shown here use a horizontal scale with $z = 0$ at the magnetic center. A sketch of the layout is shown above. The proton beam enters at an angle θ_{beam} with respect to the magnet axis. The jet is at an angle $\theta_{jet} = \theta_{beam} - \theta_{crossing}$. The vertical distance y_o from the magnet center $(z = 0, r = 0)$ to the jet axis at $z = 0$ can be chosen to minimize beam disruption. We assuming a Gaussian distribution of B'_z vs z', with a maximum value of B_o, The jet conductivity κ, density ρ, and surface tension $T_{surface}$, and the other parameters are given below:

B_o	20	T
σ'_z	.8	m
θ_{jet}	-67	mrad
y_o (without surface tension)	2	mm
y_o (with surface tension)	1	mm
κ	10^6	Ω m
ρ	13.5 10^4	kg/m^3
$T_{\rm surface}$	.456	N/m
$p_{\rm gas} = p_{\rm atmospheric}$	10^5	N/m^2

Plots are shown for

a) The axial magnetic field B_z

b) The vertical magnetic field B_y

c) The rate of change of the transverse field B_y

c) The hydrostatic pressure on the jet axis with respect to the environment outside the jet $(p_{\rm axis} - p_{\rm gas})$

d) The average deceleration of the jet Δ_v(Ave)

e) The maximum shear acceleration/deceleration of the upper/lower limits of the jet Δ_v(shear)

f) The vertical displacement of the jet due to deflecting forces y

g) The total transverse distorting forces F_{distort}

h) The resulting elliptical distortion (δx/r=$-\delta$y/r), without surface tension

1. The resulting elliptical distortion (δx/r=$-\delta$y/r), without surface tension

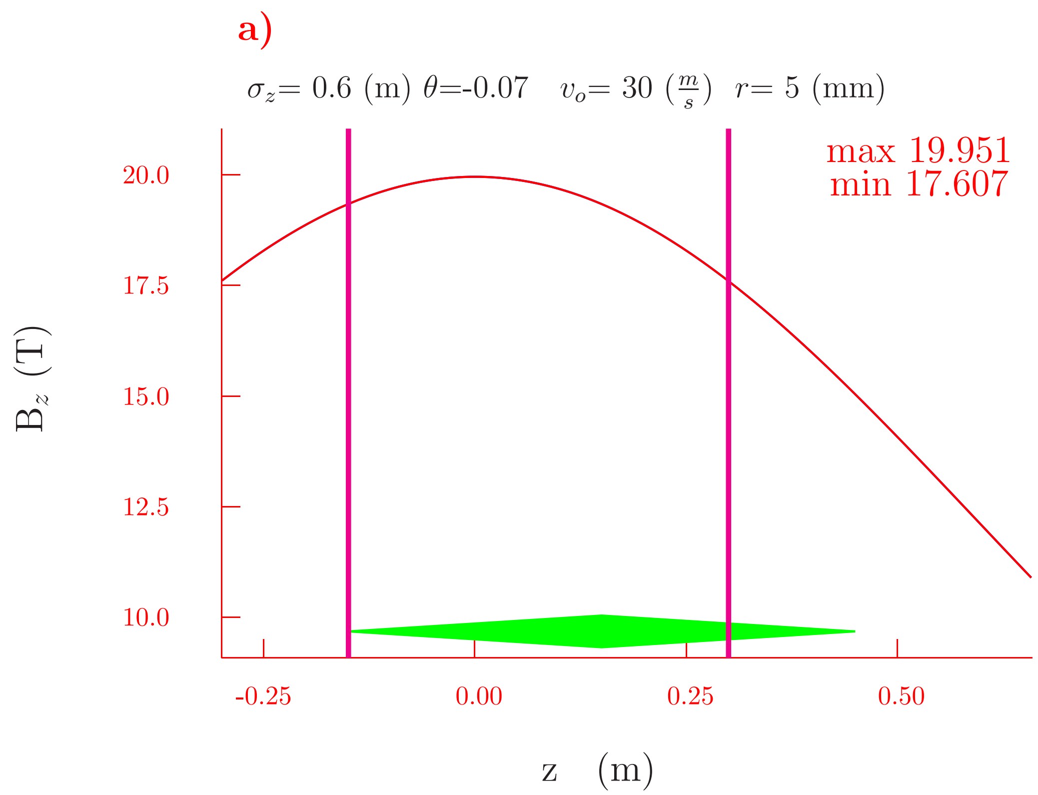
a)
σ_z= 0.6 (m) θ=-0.07 v_o= 30 ($\frac{m}{s}$) r= 5 (mm)
max 19.951
min 17.607
20.0
17.5
15.0
12.5
10.0
B_z (T)
-0.25
0.00
0.25
0.50
z (m)

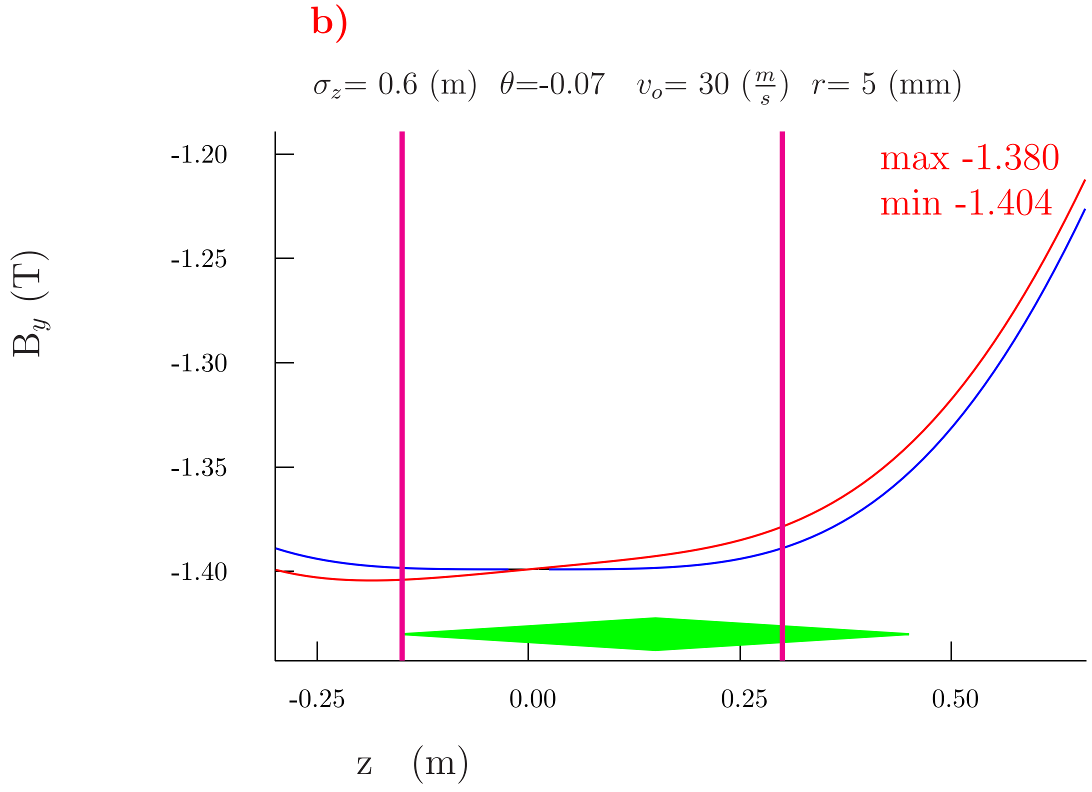
b)
σ_z= 0.6 (m) θ=-0.07 v_o= 30 ($\frac{m}{s}$) r= 5 (mm)
max -1.380
min -1.404
-1.20
-1.25
-1.30
-1.35
-1.40
B_y (T)
-0.25
0.00
0.25
0.50
z (m)

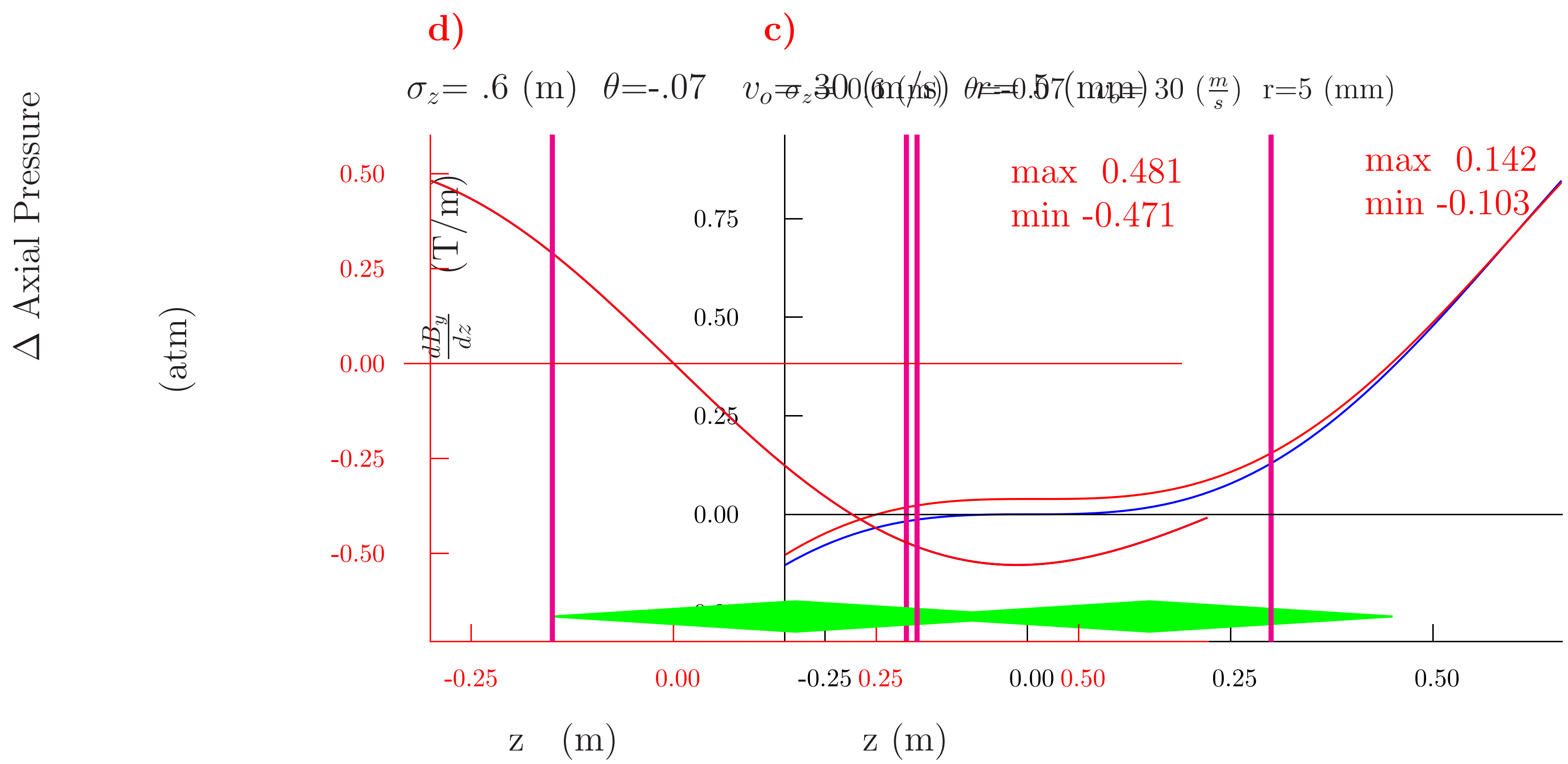
d)
c)
σz= .6 (m) θ=-.07 vo= 30 (m/s) r=.5 (mm)
σz= .6 (m) θ=-.07 vo= 30 (m/s) r=5 (mm)
max 0.481
min -0.471
max 0.142
min -0.103
Δ Axial Pressure
(atm)
dBy/dz (T/m)
0.50
0.25
0.00
-0.25
-0.50
0.75
0.50
0.25
0.00
-0.25
0.00
0.25
0.50
-0.25
0.00
0.25
0.50
z (m)
z (m)

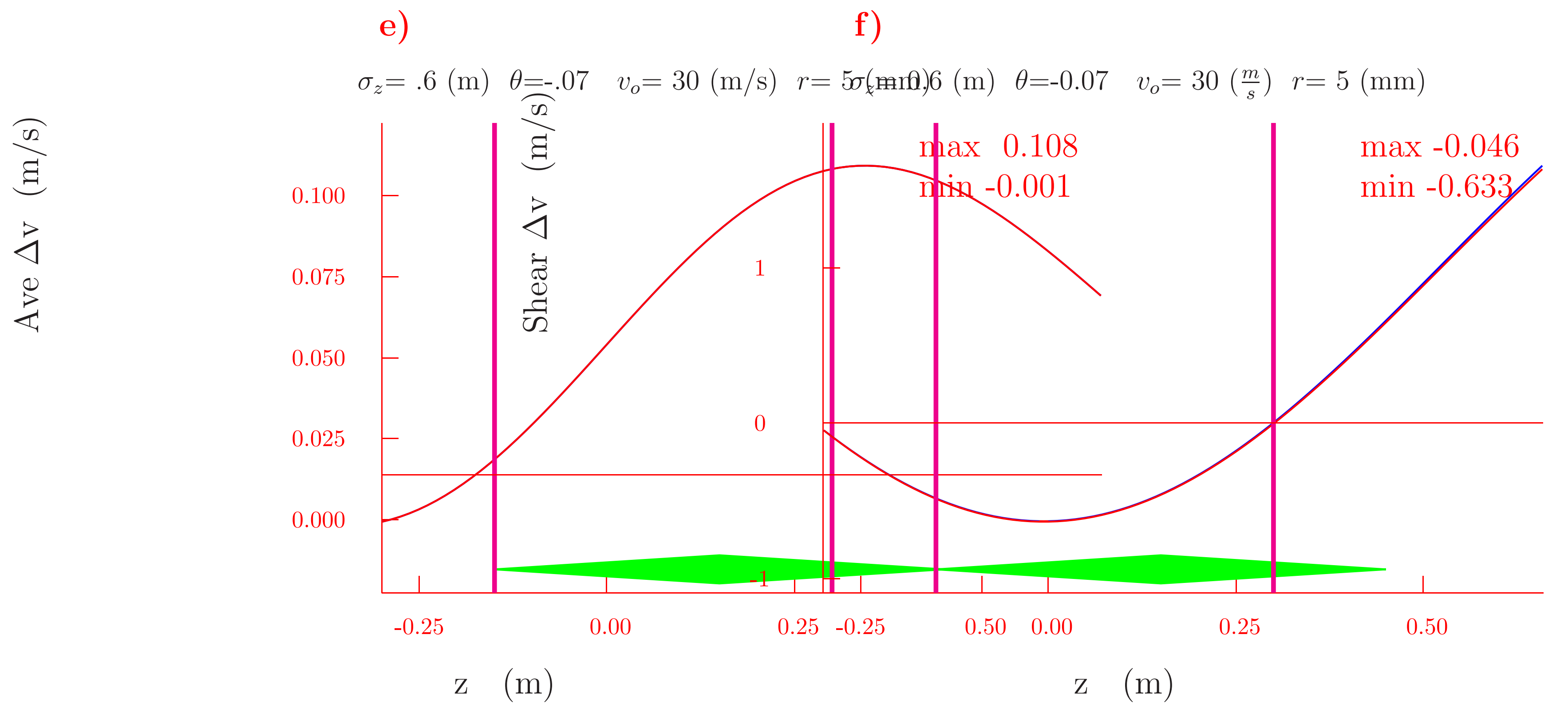

e)
σ_z= .6 (m) θ=-.07 v_o= 30 (m/s) r= 5 (mm)
Ave Δv (m/s)
0.100
0.075
0.050
0.025
0.000
-0.25
0.00
0.25
0.50
z (m)
max 0.108
min -0.001
f)
σ_z= 0.6 (m) θ=-0.07 v_o= 30 ($\frac{m}{s}$) r= 5 (mm)
Shear Δv (m/s)
1
0
-1
-0.25
0.00
0.25
0.50
z (m)
max -0.046
min -0.633

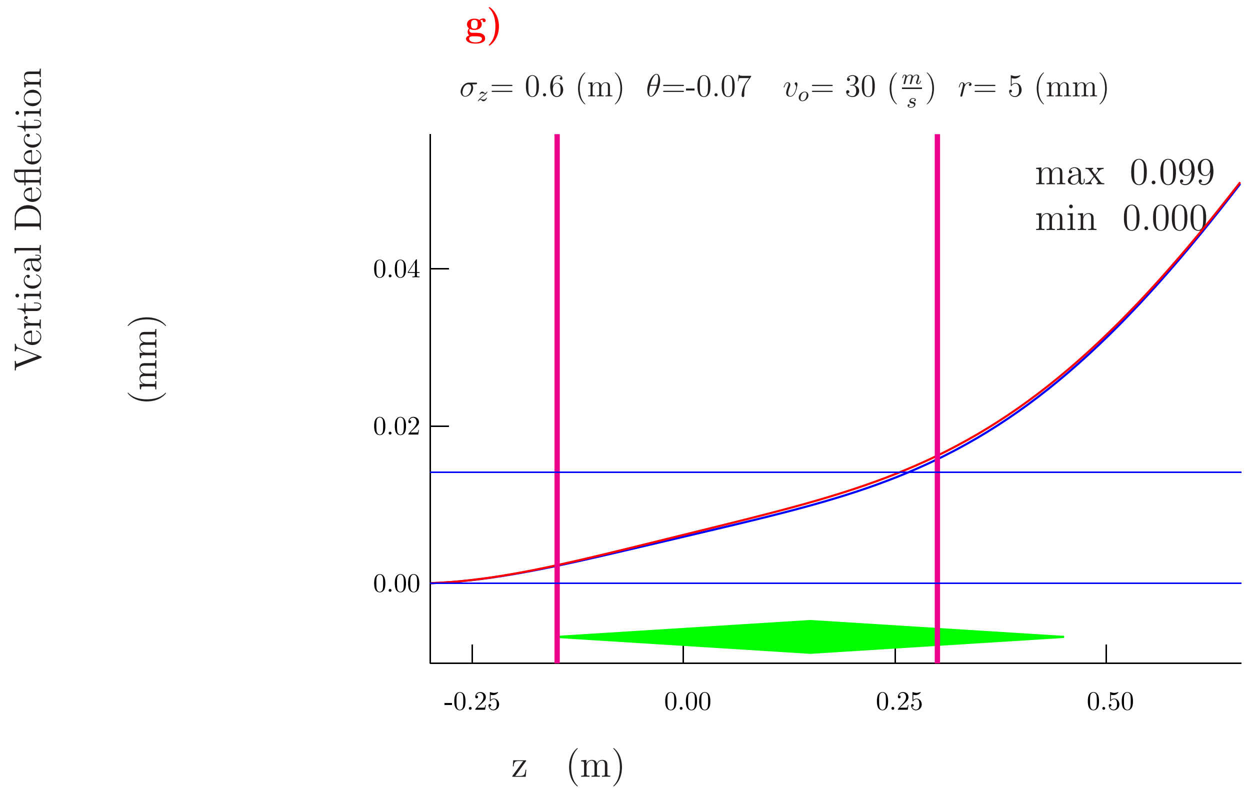
g)
σz= 0.6 (m) θ=-0.07 vo= 30 (m/s) r= 5 (mm)
max 0.099
min 0.000
Vertical Deflection
(mm)
0.04
0.02
0.00
-0.25
0.00
0.25
0.50
z (m)

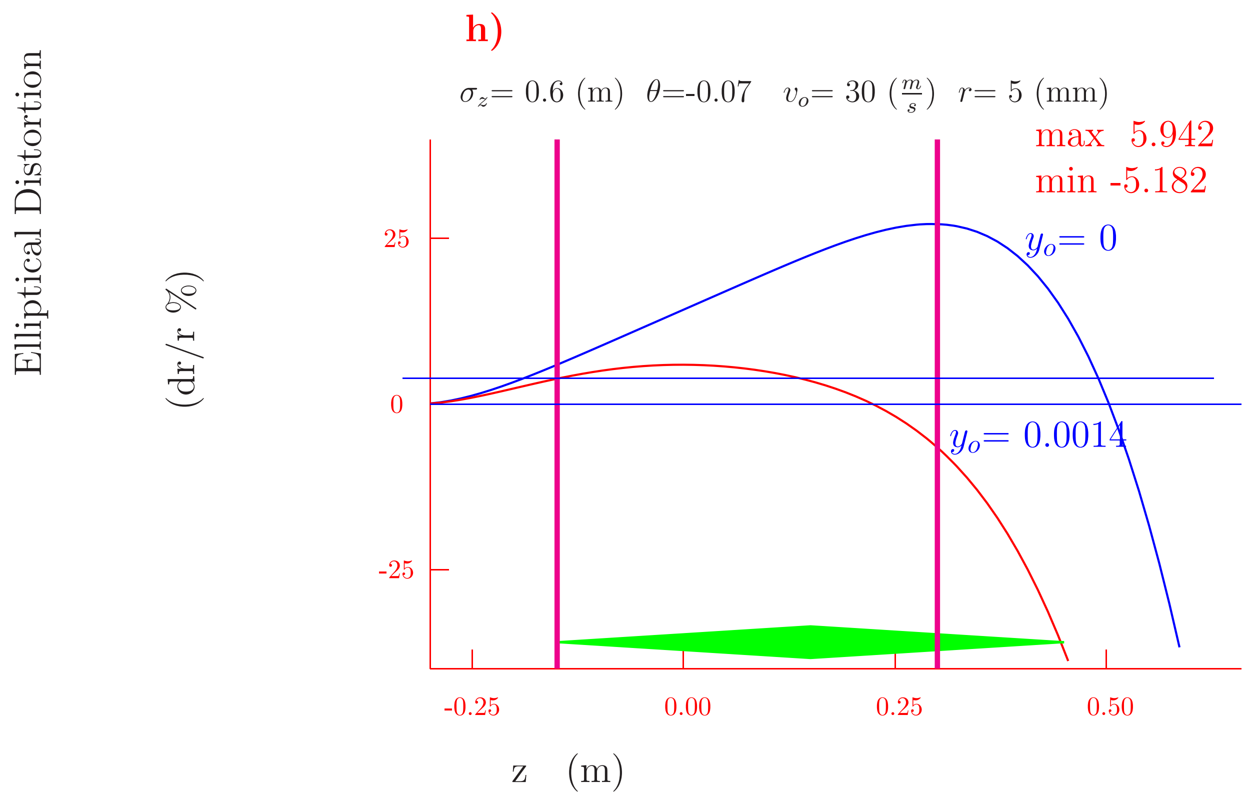
h)
σz= 0.6 (m) θ=-0.07 vo= 30 (m/s) r= 5 (mm)
max 5.942
min -5.182
yo= 0
yo= 0.0014
Elliptical Distortion
(dr/r %)
25
0
-25
-0.25
0.00
0.25
0.50
z (m)

We see that over the extent of the new jet (from - .3 to .3 m):

- The maximum axial field deviations are $+/-$ 1.25 T = 6%
- The transverse fields seen by the jet are approximately 1.4 T, and vary at the ends by only up to $+/-$ 0.01 T = $+/-$ 0.7 %. But it is this small variation of transverse field that generate axial current in the jet, leading to jet shape distortions that are the most serious constraint on the magnet design.
- The axial pressure difference has a minimum of - 0.5 atmospheres. Thus if the jet is operating in a gas (He or Argon) at a pressure of 1 atmosphere, then the minimum pressure will be + 0.5 atmospheres, and there will be no tendency to cavitate prior to the arrival of the beam.
- The maximum average deceleration of the jet is small compared to the average jet velocity: 0.11/30≈0.3%.
- The maximum decelerations (from shear forces) are also small compared to the average jet velocity: 0.7/30≈2.3%.
- The deflections of the jet are very small: 20 μm.
- The resulting calculated jet distortions (Δ width / ave width) with no jet axis displacement ($y_o = 0$) are approximately 30% without surface tension, but are reduced to 10%, by the restraint from surface tension. Both can be reduced to 6-7% by small jet axis displacements.

These disruptions are all relatively small, and should, with the fields assumed, cause no problems. But relatively small field changes can make the beam distortions uncomfortably large. It thus appears that considerations of these distortions will set the tolerances on the magnetic field shape. Tuning of these distortions can be achieved by vertical displacements of the jet, and provision for mechanically adjusting this should be considered.

5 Coil Design

6 Using Calculated Fields

Plots of the magnetic fields and derivatives needed in this calculations including the relative tilded of $\theta = 0.1$ between jet and solenoid axis are shown in Figs.2 and 3

****

Compared with a jet velocity of 20 m/sec, these are all relatively low. Earlier optimizations had called for a jet radius of 1 cm, which gave values of Δv 4 times higher, and thus more significant.

7 Conclusion

****

References

[1] `http://www.cap.bnl.gov/mumu/studyii/`

[2] K. McDonald (Ed), *An R&D Program for Targetry and Capture at a Muon-Collider Source*, Proposal to the BNL AGS Division, p.23

[3] R. Weggel, *Behavior of conducting solid or liquid jet moving in magnetic field: 1) Paraxial; 2) Transverse; 3) Oblique*, BNL report BNL-65611/CAP-220-Muon-98R

[4] **Phys. Today**, Feb 2000, p.29

[5] R. Weggel, *20 T Hybrid magnet for Study II*

[6] K. McDonald, *Damping and Radial Pinching Effects*,

`http://www.hep.princeton.edu/~mcdonald/mumu/target/radialpinch.ps`